A Combined Optimization and Decision Making Approach for Battery Supported HMGS

Carolina Marcelino, Manuel Baumann, Leonel Carvalho, Nelson Chibeles-Martins, Elizabeth Wanner, Paulo Almeida and Marcel Weil

. ***Abstract*—Hybrid micro grid systems (HMGS) are gaining more attention within the World. The balance between load and electricity generation based on fluctuating renewable energy sources is a main challenge within HMGS operation and design. Battery energy storage systems are seen as a crucial component to integrate a high share of renewable energy into a HMGS. Currently, there are very few studies in the field of mathematical optimization and multi-criteria decision analysis that focus on the evaluation of different battery technologies and their impact on HMGS design. The model proposed in this paper aims at optimizing three different criteria, namely the minimization of the electricity costs, the loss of load probability and the maximization of locally available renewable energy usage. The model is applied in a case-study in the south of Germany. The optimization is carried out using the C-DEEPSO algorithm. Results are used in an AHP-TOPSIS model using expert weights to identify the most recommendable alternative out of five different battery technologies. Lithium batteries are considered to be the best solution based on the given group preferences and optimization results.**

***Index Terms*—Smart Grids, Evolutionary Optimization, Decision Theory, Battery Energy Storage Systems, Renewable Energy.**

TABLE I
ABBREVIATION LIST

AC	Alternating Current
AHP	Analytic Hierarchy Process
Al	Aluminum
BESS	Battery Energy Storage Systems
BoP	Balance of Plant
CCA	Classic Compensatory Approaches
C-DEEPSO	Canonical Differential Evolutionary Particle Swarm Optimization
CIS	Closeness to the Ideal Solution
Co	Carbone
COE	Cost of Electricity
CR	Consistency Ratio
DC	Direct Current
DE	Differential Evolution
DoD	Depth of Discharge
EVM	Eigenvector Method
GCI	Geometric Consistency Index
HMGS	Hybrid Micro Grid System
IC	Initial Cost
LFP	Lithium Iron Phosphate
LOLP	Loss of Load Probability
MCDA	Multi-Criteria Decision Making Analysis
Mn	Manganese
NaNiCl	Sodium Nickel Chloride
NaS	Sodium Sulfur battery
NCA	Lithium Nickel Cobalt Aluminum Oxide
Ni	Nickel
OA	Outranking Approaches
PSO	Particle Swarm Optimization
PV	Photovoltaic
RGMM	Geometrical Mean Method
RS_{factor}	renewable energy sources
SoC	State of charge
TOPSIS	Technique for Order Preference by Similarity to Ideal Solution
VRLA	Valve Regulated Lead Acid batteries

I. INTRODUCTION

Recently there is a global need for sustainable energy. Part of this energy is intended to be produced by micro-generation systems in a decentralized way. Market-driven policies are increasingly focused on promoting the deployment of micro-generation systems to meet customer needs. This change, however is proving to be a challing task namely for those who choose to produced their own electricity based solely on the renewable resources locally available, such as wind or solar radiation. Hybrid microgrid systems (HMGS) are seen as a viable solution for this problem, since these local distribution systems are composed of one or more distributed energy sources and include centralized systems for controlling the demand, the storage devices and the generation sources. In addition, HMGS are capable of not only operating autonomously but also become connected to the public grid.

The increasing market rollout of fluctuating decentralized renewable energy resources such as photovoltaic (PV) and wind power represents a challenge for the grid stability in Germany within the so called "Energiewende" - Energy transition. HMGS are seen as a possibility to integrate such distributed electricity sources into a local electricity network. These systems can be described as clusters of small generators, loads, demand response and battery energy storage systems (BESS) connected through a local electricity network, controlled by a power management system (24). The interconnection and coordination of multiple HMGS can be achieved within a smart distribution grid (13). A simplified scheme of a HMGS, including BESS, is shown in Fig. 1.

A major issue of such HMGS is to guarantee at every moment the balance between generation and load, to keep frequency and voltage within admissible levels. BESS can

C. G. Marcelino and P. Almeida are working at the Centro Federal de Educação Tecnológica de Minas Gerais (CEFET-MG) on Intelligent Systems Laboratory, Belo Horizonte, Brazil. E-mail: {carolina, pema}@lsi.cefetmg.br

L. M. Carvalho is working at INESC TEC, Institute for Systems and Computer Engineering, Porto, Portugal.

E. Wanner is working at Aston University, School of Engineering and Applied Sciences, Birmimgham, UK and at CEFET-MG, Belo Horizonte, Brazil.

N. Chibeles-Martins is working at the Centro de Matemática e Aplicações (CMA) Universidade Nova de Lisboa (UNL), Lisboa, Portugal.

M. Baumann and M. Weil are working at the Institute for Technology Assessment and Systems Analysis (ITAS) on Karlsruhe Institute of Technology (KIT), Karlsruhe and Helmholtz-Institute for Electrochemical Energy Storage (HIU), Ulm, Germany and Universidade Nova de Lisboa (UNL), Lisboa, Portugal. E-mail: {manuel.baumann, marcel.weil}@kit.edu

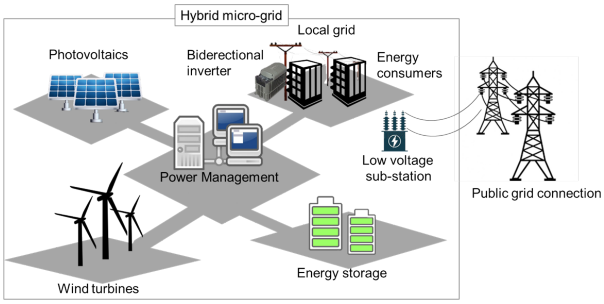

Fig. 1. Simplified configuration of a HMGS including BESS. Extracted from: (4).

solve this challenge by responding within seconds to load and generation changes. There are several battery technologies available, each with their advantages and disadvantages (e.g. high efficiency vs. low cost etc.). Thus, it is crucial to match technology properties with the specific requirements determined by the HMGS design goals.

The specialized literature highlights three major goals for HMGS design: 1) to minimize the cost of electricity (COE) per electricity unit generated; 2) to minimize the Loss of Load Probability (LOLP) or breakdowns; 3) to maximize the share of renewable energy sources in the generation mix (RS_{factor}) (24; 2; 5). Selecting the right battery system represents, in this way, a multi-objective decision problem, that cannot be achieved by a single technology and that requires trade-offs to be considered. Furthermore, the decision to implement a certain system design involves several stakeholders that may have different views and interests on the task (e.g. utility vs. customers).

These questions must be taken into account when HMGS components, such as renewable energy systems and a BESS technology, are selected. Several attempts have been carried out to design and operate such electrical systems in an efficient and sustainable way. The work described in (30) uses a Particle Swarm Optimization (PSO) method to optimize the components of a HMGS and to maximize the total net present worth. This is achieved by optimizing the size of BESS, PV units and wind generators over the considered project planning horizon. Similar approaches can be found in (2), (21) and (29).

Other attempts to HMGS design come from the area of multi-criteria decision making analysis (MCDA) in combination with optimization techniques (22; 39). Especially, participative MCDA methods can be used to obtain preferences regarding the potential benefits and costs to define an optimum development strategy for HMGS (22). Several MCDA methods available for this purpose have been described in (18) and (41).

However, there is a lack of detail when it comes the selection of the BESS technology since this is critical component for HMGS design. This paper proposes the use of the metaheuristic Canonical Differential Evolutionary Particle Swarm Optimization (C-DEEPSO) for selecting the best BESS technology by optimizing the aforementioned HMGS attributes (COE, LOLP and RSfactor) simultaneously. Results are then used in the Analytic Hierarchy Process (AHP) and the Technique for Order Preference by Similarity to Ideal Solution (TOPSIS) to find the most recommendable BESS option using weights provided by five stakeholders.

This paper is organized as follows: Section 2 deals with the HMGS modeling, the techno-economic assumptions and the optimization model for HMGS design. The C-DEEPSO algorithm is presented in Section 3. The AHP+TOPSIS methodology is described in Section 4. Section 5 discusses the case study, experiments and results. Finally, Section 6 presents the conclusions and gives an outlook for future work.

II. Hybrid Micro Grid System modeling

The model for HMGS design optimization proposed in this paper is based on a reference model described in (5). The aim of this hourly-based optimization is to reduce COE and LOLP, as well as to increase the share of the electricity produced with local renewable energy sources (RS_{factor}). This is carried out by optimally adjusting the installed capacity of the PV panels, of the wind turbines, of the diesel generators, and of the BESS based on the hourly demand and the availably primary energy resources (solar radiation and wind speed). The original model described in (5) was solved using a PSO algorithm based on a generic battery technology with a multiobjective approach.

This model is reformulated into a grid-connected HMGS, wherein the BESS operation is set to minimize the amount of excess energy produced locally. Furthermore, five different BESS technologies are included in the optimization process to explore their impact on the overall system performance taking into account the three optimization goals. The results are used in a multi-criteria decision making approach using AHP+TOPSIS to determine which of the system designs is the most recommendable regarding the stakeholders' perspective. This section provides the details about HMGS optimization model. An overview of the entire approach is given in Fig. 2.

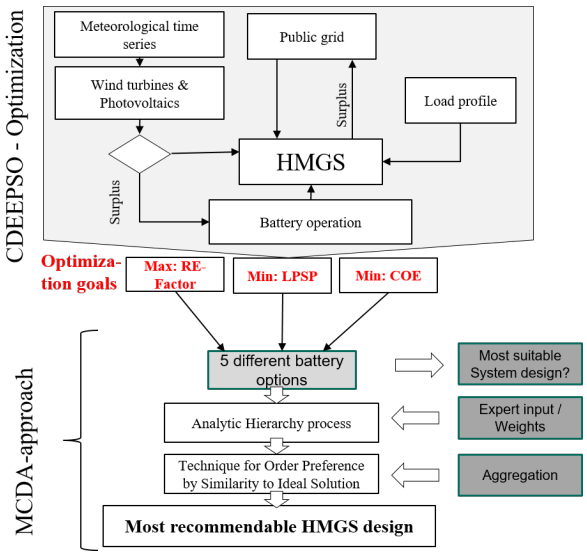

Fig. 2. Overview of the entire approach.

A. Battery storage technologies for HMGS

Electrochemical energy storage is seen as a valuable option to facilitate the integration of renewable energy and defer grid expansion investments. BESS can provide ancillary services, load balancing, voltage stabilization and service restoration after a blackout. These systems are composed by several cells stacked in series and in parallel to achieve the desired capacity. Battery management systems are used to control the charge and discharge of the BESS and to maximize its lifetime.

The BESS technologies considered in this work are Li-Ion batteries (Lithium Iron phosphate - LFP and Lithium Nickel Cobalt Aluminum Oxide - NCA), valve regulated lead acid batteries (VRLA) and two high temperature batteries (Sodium Nickel Chloride (NaNiCl) also referred as Zebra battery and Sodium Sulfur battery (NaS)). Li-Ion batteries are produced with various anode and cathode combinations resulting in different performance characteristics. The anodes currently use graphite or lithium salt of titanium oxide as active material. Cathode active material can be Co-dioxide, Ni, Co, Al or Mn composite oxides, Mn spinel oxide or iron phosphate (38).

Li-Ion batteries can achieve high charge-discharge efficiency levels. In contrast, lead-acid BESS are still the cheapest option, while losing ground to cheap Li-Ion chemistries such as the ones based on iron phosphate. Li-Ion batteries have already overtaken all other battery technologies regarding globally installed capacity (3). High temperature batteries, such as NaS and NaNiCl, can operate in the range of 270 to 350^oC with electrodes in a liquid state (36). They also offer certain advantages regarding cost and recycling. More information about different battery storage systems can be found in (36; 7).

B. HMGS Design Goals

This section describes the optimization model for HMGS design, which has been discussed in depth in (5). Table II provides an overview of the main parameters of the model.

TABLE II
PARAMETERS USED IN HMGS MODEL.

Parameter	Description
COE	total costs in electricity
$LOLP$	loss of power supply probability
$Total_{costs}$	total costs in HMGS
P_{load}	power consumption
P_{pv}	power production by PV
P_{wind}	power production by wind generator
$P_{soc_{min}}$	minimun power compensation by battery
P_{grid}	power from public grid

The model used in this paper is based on a bi-objective problem with the aim of minimizing COE and LOLP. According to (20), COE can be obtained in terms of \$/kWh, by using the following equation,

$$COE = \frac{C_{total}}{\sum_{h=1}^{h=8640} P_{load}(h)} \times CRF, \tag{1}$$

in which C_{total} are costs of installation, maintenance, operation and replacement of HMGS components. Power consumption over time (simplified 8640 hours = 24h $\times$ 30 days $\times$ 12 months – (5)) is given by P_{load}. The CRF is a ratio to calculate the present value of the costs for a given planning horizon taking into consideration the interest rate (5; 20).

The value C_{total} represents the sum of system initial cost (IC) - personnel cost, installation and connections - periodic costs PW_p - maintenance of PV panels, maintenance of wind generator, among others, and non-recurrent cost PW_{np} characterized as a cost of BESS replacement and others (see (20)).

A new factor, degradation cost c_d presented in (23), is added in the computation of C_{total} to provide a more realistic approach. This factor considers the BESS degradation in terms of available cycle lifetime L_c and the energy storage capacity, E_s, at a certain depth of discharge (DoD) related to the total BESS cell costs, c_{bat}, as indicated in Eq. (2),

$$c_d = \frac{c_{bat}}{L_c E_s DoD}. \tag{2}$$

Then, in this model, C_{total} is obtained by using Eq. (3),

$$C_{total} = IC + PW_p + PW_{np} + \sum_{h=1}^{h=8640} c_d. \tag{3}$$

Statistical techniques and chronological simulation approaches can be used to calculate the loss of load probability (LOLP). LOLP is expressed by Eq. (4),

$$LOLP(\%) = \frac{\sum P_{load} - P_{pv} + P_{wind} + P_{dch} + P_{grid}}{\sum P_{load}}, \tag{4}$$

in which P_{load} is the hourly power consumption, P_{pv} and P_{wind} are the power generated by PV and by the wind generator. P_{dch} is the discharge power of the battery, P_{grid} is the power withdrawn from the public grid and P_s is the power surplus generated. The amount of energy generated by renewables is calculated as,

$$RS_{factor}(\%) = \frac{\sum P_{pv} + P_{wind} + P_{dch} - P_s}{\sum P_{load}}. \tag{5}$$

C. Optimization Model

A simple approach to simultaneously minimize COE and LOLP is to use a linear scalarization of the two objectives to create a weighted-sum mono-objective optimization problem. In this scalarization, the weights of the mono-objective functions are associated with the importance of each objective (5; 11; 27; 12; 31).

For every set of weights, which represent the relative importance of each objective function, a solution for the corresponding mono-objective problem can be obtained. In a well-posed weighted mono-objective problem, each solution of the mono-objective problem is a single point in the Pareto front (8). The weighted-sum mono-objective problem is given by Eq. (6)

$$fitness = min \left\{ \sum_{i=1}^{k} w_i \frac{f_i(x)}{f_i^{max}} \right\}, \tag{6}$$

$$\text{with } w_i \geq 0 \text{ and } \sum_{i=1}^{k} w_i = 1,$$

$$\text{subject to: } min\ g_i(x) \geq 0\ for\ i \in \{1, ..., m\},$$

in which k is the number of objectives, w_i are the weights for each objective, x is the vector of decision variables, f is the objective function and f_i^{max} is the upper bound of ith objective function. Functions $g_i(x)$ are the inequality

constraints. In this work, the objective functions, COE and LOLP, are aggregated into a mono-objective function using 0.5 as the weight for each goal as in (5). Therefore, the weighted-sum objective function adopted in this work is,

$$min\ f' = 0.5 \times COE + 0.5 \times LOLP + \rho \sum_{i=1}^{n} max[0, RS_{factor}]^2, \quad (7)$$

in which the RS_{factor} constraint is included using the penalty factor (ρ).

III. The C-DEEPSO algorithm

The metaheuristic Canonical Differential Evolutionary Particle Swarm Optimization (C-DEEPSO), proposed by (26), is a method that merges distinct principles of evolutionary computation and swarm intelligence. C-DEEPSO employs mutation operators, recombination and selection to create new solutions as most available population metaheuristics do. Unlike its predecessor algorithm, the DEEPSO algorithm (6), this technique uses the mutation operator of the Differential Evolution (DE) algorithm (37). This operator uses 3 vectors for the process, which ensures greater diversity to the search. Table III shows the main parameters of C-DEEPSO algorithm.

TABLE III
Parameters used in C-DEEPSO.

Parameter	Description
t	is the current generation
X	is the current solution
X_{gb}	is the best solution in generation
V	is the velocity of solution
F	is disturbance rate
$*$	parameter is subjected to the mutation process
C	is a diagonal matrix of random variables sampled at each iteration (with probability P of communication)

Similar to DE, the mutation operator in C-DEEPSO has a disturbance rate F associated, that usually lies within the [0, 1] range. This is done to assure the swarm is gradually refined by the best fitness solutions in every generation, until a certain stopping criterion is reached. Generation of new solutions in C-DEEPSO is carried out through the recombination of the current solutions and the selection of the best solutions found in the swarm. Recombination is obtained by using Eq. (8) and Eq. (9),

$$X_t = X_{t-1} + V_t, \quad (8)$$

$$V_t = w_I^* V_{t-1} + w_A^*(X_{st} + F(X_r - X_{t-1})) + w_C^* C(X_{gb}^* - X_{t-1}), \quad (9)$$

in which *st* is DE/best/1/bin strategy by DE algorithm (37). The variables w_I, w_A and w_C are weights on the inertia, assimilation and communication, respectively. The superscript $*$ indicates that the corresponding parameter/quantity undergoes evolution under a mutation process.

The term C represents a matrix that has a communication probability P (operation can be viewed in Fig. 3). This matrix is inspired by the "*stochastic star communication topology*" (28). This technique provides that each solution of the whereabouts of the global best-so-far point is randomly controlled by P.

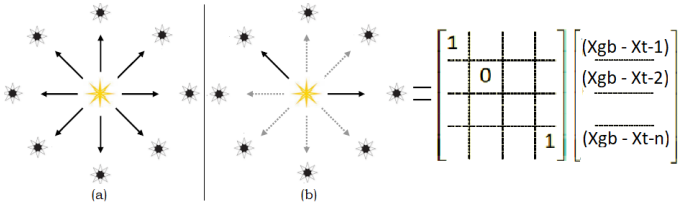

Fig. 3. Legend: star communication (a) and stochastic star topology (b). The binary matrix C is obtained using the rule: randomly generate N values within the [0,1] interval for each dimension inside in each solution. The randomly generated value is compared to communication rate P. If this random value is greater then P, the element C_{ij} of C matrix receives 0, otherwise 1.

The effect is that a solution cannot use the information from the global best in some iterations (as in selfish or cognitive model) and takes it into account in other iterations. C-DEEPSO has a memory mechanism, called $Memory\ B$. The central idea of this mechanism is to save a subset of best solutions of the last iteration in an archive with a rate in % of population, which encloses not only solution, but also the corresponding fitness. So, this archive is used to obtain the term X_r that is a solution different from X_{t-1} that can be obtained accordingly:

1) S_g-rnd: sampled as an uniform recombination from the individuals of the current generation;
2) P_b-rnd: sampled as an uniform recombination within Memory B, and
3) S_gP_b-rnd: obtained by an uniform recombination from results of S_g-rnd and P_b-rnd.

When using S_gP_b-rnd, an uniform recombination from different solutions is used to obtain X_r, and the reversion of the position of X_r and X_{t-1}, in Eq. (9), is done for every dimension of the search space, when X_{t-1} is better than X_r. Typically, mutation in weights w follows the rule described by Eq. (10),

$$w^* = w + \tau \times N(0,1), \quad (10)$$

in which τ is the mutation rate that must be set by the user. $N(0,1)$ is a number sampled from the standard Gaussian Distribution. Note that the weight must be non-negative and lower than 1. The initial weight matrix is randomly generated in [0,1] interval. In Eq. (9), generation of the best solution, X_{gb}, is also mutated.

This position is slightly attracted by the movement in the search space also using a Gaussian distribution. This is done to prevent the population to be trapped in a particular region, which normally occurs when a certain solution becomes dominant over the others. Thus, the mutation in X_{gb} is obtained by Eq. (11),

$$X_{gb}^* = X_{gb}[1 + \tau \times N(0,1)]. \quad (11)$$

Algorithm (1) presents a simplified execution cycle of the C-DEEPSO.

Algorithm 1: *Pseudocode of C-DEEPSO.*

begin
- **Step 1: Set** values of control parameters of C-DEEPSO - Population size NP, Mutation rate τ, Communication rate P, Memory rate MB and Dimension (D) ;
- **Step 2: Set** the generation number $t = 0$ and randomly initiaze a population of NP individuals;
- **Step 3: Evaluate** the current population, NP;
- **Step 4: Update** the global optimum, X_{bg};
- 1 **while** *stopping criterion is not satisfied* **do**
  - 2 **for** *each individual i that belongs to population NP* **do**
    - **Calculate** X_r using the strategy, $S_g P_B$-rnd;
    - **Copy** the current individual X_{t-1};
    - **Mutate** the strategy parameters w_I, w_A, w_C using Eq. (10);
    - **Mutate** X^*_{gb} using Eq. (11) ;
    - **Apply** movement rule in current individual X_{t-1} using Eq. (9);
    - **Evaluate** the current individual X_t and your copy;
    - **Select** the individual with better fitness to proceed next population ($NP + 1$). **Using for example Stochastic Tournament*;
  - **Update** the best individual X_{bg} and memory MB;
  - $t = t + 1$

IV. Multi-Criteria Decision Analysis

MCDA is considered as a branch of operation research which deals with decision problems involving multiple criteria. In general, MCDA can be separated into classic compensatory approaches or multi-attribute utility theory methods (CCA, or American school) and outranking approaches (OA, or European school) (17; 19; 25). All MCDA methods have their theoretical hypothesis and are usually adequate for different decision problems. A good comparison of OA and CCA is given in (17) which also offers some recommendations for a proper MCDA method choice.

A. AHP and TOPSIS

MCDA methods can be roughly schematized by a construction phase (input data and the modeling phase that includes the interface to stakeholders) and an exploitation phase (the aggregation and calculation leading to recommendations). The Analytic Hierarchy process (AHP) is used for the construction phase and the Technique for Order Preference by Similarity to Ideal Solution (TOPSIS) is considered as a suitable approach for the exploitation phase which will be reasoned in the following.

AHP is used here as it is considered to be user friendly and understandable from a participant perspective due to a intuitive way of criteria comparison. It represents a non-linear framework for carrying out both deductive and inductive thinking, considering several factors simultaneously, allowing for trade-offs to arrive at a synthesis (34). The method requires a hierarchical or a network structure that represents the decision problem (33). This is simply done by decomposing and structuring the given decision problem into different levels within a hierarchy. At the top of this hierarchy, the general objective of the decision process (e.g. choice of technology or policy) remains.

Criteria related to the problem can be found below this level and can be further decomposed. Competing alternatives are located at the bottom below the lowest-level criteria (33; 16). Pairwise comparisons based on a 1-9 scale of absolute numbers have to be carried out to gather the relative importance of each criterion based on this hierarchical structure. The basic question for pairwise comparisons is: *how dominant is one criterion in relation to another criterion?* This comparison expresses the preference to a specific attribute assigned by a stakeholder (32). The relative importance of two compared criteria is scaled in a fixed continuum from 1 to 9 as depicted in Table IV.

TABLE IV
AHP pairwise comparison scale

1	Equal importance	Two criteria contribute equally to objectives
3	Slightly more important, weak moderately	One criteria is slightly favored against another
5	Moderately more important, essential importance	One criteria is moderately favored against another
7	Strongly more important, strong importance	One criteria is strongly favored over another
9	Extremely more important, absolute importance	One criteria is favored over another with the highest possible order of affirmation
2, 4, 6, 8	Intermediate values between the two adjacent scale values	Used to represent compromise between priorities listed above

Priorities are derived when all pairwise comparisons have been carried out by the participants. Most common methods to calculate priorities are the Geometrical Mean Method (RGMM) and the classic Eigenvector method (EVM). It is considered that RGMM does as well as EVM or even better than it, regarding rank reversal and other aspects (9).

It is possible that judgments in the pairwise comparison matrix are totally consistent or not (1). Inconsistency is a consequence of the attempt to derive a priority through the comparison of two objects at the same time. These objects may be involved in several comparisons on a non-standardized scale, where relative values are assigned as a matter of judgment where inconsistency may occur. A consistency ratio (CR) is thus introduced in classic EVM to exclude non consistent comparisons (34). The geometric consistency index (GCI), proposed by (9), provides approximated thresholds for RGMM and is used in this work instead of CR, which is only valid for EVM (1). High GCI values reflect inconsistency and low ones, the opposite. These thresholds are calculated for each participant by the use of Eq. (12),

$$GCI = \frac{2}{(n-1)(n-2)} \sum_{i<j} \log^2 e_{ij}, \tag{12}$$

in which $e_{ij} = a_{ij} w_j \setminus w_i$ is considered as the error obtained when the ratio $w_i \setminus w_j$ is approximated by a_{ij}. The following GCI values provided by (1) that correspond to a CR$\leq$0.1 are: $GCI = 0.31$ for $n = 3$, $GCI = 0.35$ for $n = 4$ and $GCI = 0.37$ for $n > 4$ should not be exceeded.

TOPSIS represents an efficient and easy way for criteria aggregation. It is based on the idea of (18) that a chosen alternative should have a minimum distance to the positive ideal solution A^*, and a maximum distance to the negative ideal solution A^-.

Finally, the computation of the closeness to the ideal solution (CIS) to rank the alternatives is done by using Eq. (13):

$$CIS_i = \frac{D_i^-}{D_i^* + D_i^-} \qquad i = 1, 2, ..., n. \tag{13}$$

The best solution is presented by $CIS_j^* = 1$ if $(A_j = A^*)$ and the worst by $CIS_j^* = 0$ if $(A_j = A^-)$. Ranking is carried out by the descending order of CIS_j, where the highest value represents the better performance (42). TOPSIS inhibits the danger of rank reversal (40; 15). Two fictitious alternatives including values $\{min_c\}$ and $\{max_c\}$ are thus introduced following the recommendations of (15). These values remain fixed so any evaluation in reference to them cannot change.

V. Case study and battery modelling

A generic region in the south of Germany is used as a hypothetical case study in this paper. Yearly time series for the typical residential demand, solar radiation (35), hourly wind speed and ambient temperatures (10) serve as model inputs. The wind velocity (m/s), solar radiation (W/m^2) and load (kW) data series are used as system input for the period of one year and are depicted in Fig. 4.

A test scenario with a maximum number of 100 households is used in the simulation. The HMGS model includes the following economic parameters partially available in (5):

- AC-DC inverter: efficiency = 96%, life time = 15 years and initial cost = $ 771.6 $kW;
- PV: PV regulator efficiency = 95%; life time = 24 years; initial cost = 1800 $/kW, rated power = 7.3 kW and PV regulator cost = $1500;
- Wind: rated speed = 12 m/s, rated power = 30kW, price = 2869.2 $/kW, life time = 24 years, swept area = 113.1 m, wind regulator cost = $1000, blades diameter = 12 m, efficiency = 95%, cut out = 20 m/s and cut in = 3 m/s;
- Economic parameters: discount rate = 6%, inflation rate = 1.4%, O&M+running cost = 20% and project life time = 24 years;
- Electricity from grid = Electricity end user price of 34 $ct/kWh.

Techno-economic values and performance curves for small wind turbines are taken from (14). Inverter costs are scale dependent and are based on (3). Table V gives a brief overview of the main techno-economic characteristics of the considered BESS, based on a battery database with over 5.000 data points for 14 different BESS technologies (36; 3). The investment costs of BESS include the cells in $/kWh, and the Balance of Plant (BoP), in $/kW, which includes auxiliary devices, communications and control equipment. Other costs are related to installation, permitting, and commissioning of the BESS (3).

VI. Experiments and results of the HMGS

This section presents the HMGS optimization results based on C-DEEPSO. Using the results, a ranking for the five considered BESS technologies is given, based on the weights given by 5 stakeholders using a AHP-TOPSIS approach.

TABLE V
Techno-economic input data for BESS within the considered HMGS based on average values (36; 3).

Factor	Unit	VRLA	LFP	NCA	NaNiCl	NaS
Cost	$/kWh	276.432	370.644	255.0	264.36	361.2
Cycles	-	1400	5000	3000	3000	3250
Efficiency	%	77	92	92	86	85.5
Lifetime	years	18	10	10	14	13.5
BoP	$/kW	374	374	374	374	374
Other cost	$/kW	328	328	328	328	328

A. HMGS results by C-DEEPSO

An experiment was performed with the use of a test BESS (efficiency = 85%; life time = 12 years; initial cell cost = 280 $/kWh; rated power = 200 kWh) to check the performance of the C-DEEPSO algorithm. Each solution inside the algorithm has 4 dimensions with a lower and upper bound of: nominal power of the PV [10,150] kW; autonomy grade for the BESS [1,3] $hours$; number of wind turbines [1,10] $units$ and nominal power of the public grid [10, 200] kW. The population was randomly initialized using the lower and upper bounds of the optimization problem, according to each of the characterized dimensions.

A movement equation (see Eq. 9 in Section III) is applied to find the initial velocity according to: $V_0 = v_{min} + (v_{max} - v_{min}) \times rand(1, D)$ in which, the minimal velocity is $v_{min} = upper_{bound} - lower_{bound}$, the maximal velocity is $v_{max} = |v_{min}|$ and D is the dimension problem. The empirical initialization parameters of the algorithm are given through: τ (communication rate) = 0.9, P (mutation rate) = 0.5, size of population (NP = 50), MB (size of memory archive) = 10% of NP, maximum number of generations (t = 30) and dimension of the search space (D = 4). The use of C-DEEPSO enabled an analysis of the energy dispatch behavior of all generation units within the proposed microgrid system. The entire simulation procedure is given in Algorithm (2).

Algorithm 2: *Pseudocode of Simulation model.*

begin
- **Step 1:**;
- **Load** meteorological data (wind speed, radiation, temperature - during one year); components characteristics; economic values;
- **Set** the initial parameters of C-DEEPSO;
- **Set** the bounds of decision variables;
- **Step 2: Execute** C-DEEPSO algoritm;
- **Set** the position and velocity randomly of first generation and them apply the fitness function to find the optimized fitness value;
- **Step 3: Return** optimized values found for COE, LOLP and RS-Factor;

Resulting optimum renewable generation capacities are as follows: 150 kWp for PV and 240 kW installed wind power capacity. A critical factor is the BESS capacity which represents a trade-off between the named optimization goals COE, LOLP and RS-Share. A test case is thus calculated within a capacity range of 100 to 700 kWh. For this, C-DEEPSO was run 30 times in each size within the named [100, 700] interval. Average results showed that LOLP remained nearly the same for all tested storage sizes (< 0.1 %).

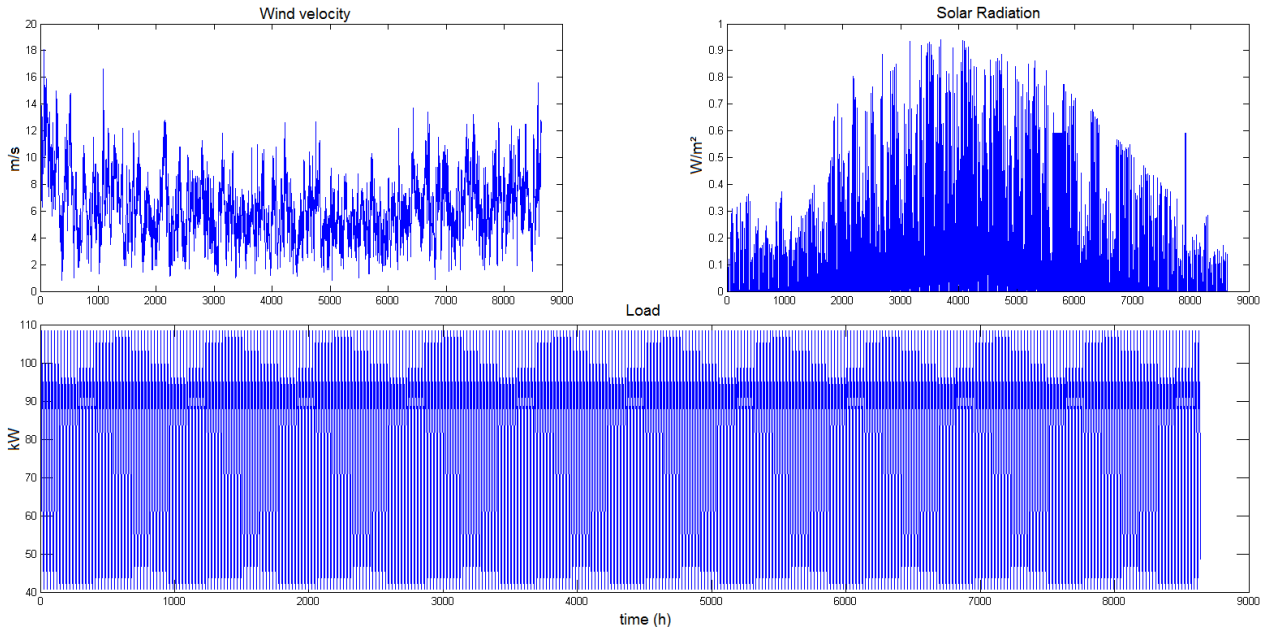

Fig. 4. Series of data representing the inputs to the HMGS model. The average annual wind speed is in the range of [1,6]m/s. The solar radiation present in this area is low and is around [0,1] W/m^2. The load demand was generated with data from 24 hours to 100 houses and replicated over the one-year.

The results depicted in Fig. 5 represent a trade-off analysis between the remaining COE and RS_{factor} based on TOPSIS using equal weights. It can be seen that the optimum BESS size can be found at a storage capacity of 200 kWh for the considered HMGS. An excerpt of the HMGS operation for different weeks in summer and winter as a result of C-DEEPSO optimization is given in Fig. 6. It can be observed how the BESS is charged and discharged at least once over the depicted period.

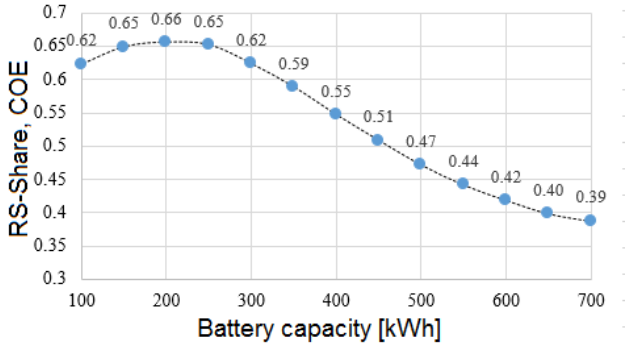

Fig. 5. Trade-off analysis regarding RS_{factor} and COE for different battery storage capacities.

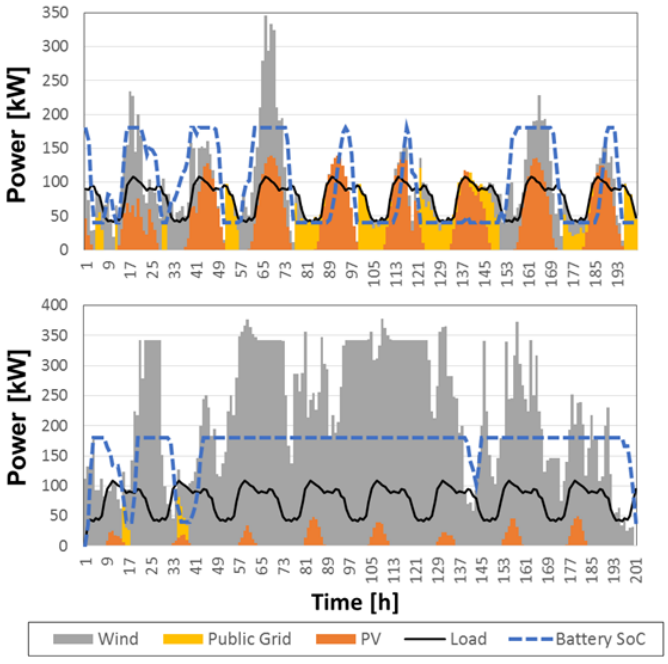

Fig. 6. Excerpt of system operation behaviour for summer (upper graph) and winter (lower graph) - Input data: wind, solar radiation and load.

The HMGS withdraws energy from the public grid when there is not enough electricity available from PV, wind and BESS. It can be clearly seen how PV contribution surpassed load in summer. The same comes true for Wind power in winter where wind velocities can become very high. This leads to a complementary situation regarding the usage of wind power and PV. The State of charge (SoC) indicates that, in summer, the BESS was utilized almost on a daily basis and only a few times in winter. The resulting total annual energy shares provided by PV, wind turbine, battery systems, surplus and public grid over a year are depicted in Fig. 7.

The HMGS can be operated at the lowest cost of 33 $ct/kWh in a way that 61% of the demanded energy is supplied by renewable sources, including the 3% share from BESS. A share of 30% is provided by the public grid to cover local demand. The surplus of 9% indicates the amount of

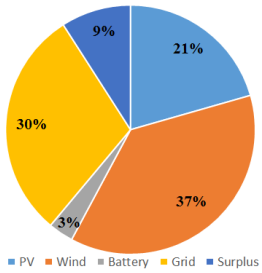

Fig. 7. Total annually generation share: wind, solar radiation, surplus and load.

renewable energy that cannot be used locally. Generally, the occurrence of surplus occurs when renewable sources are already supplying the demand and the BESS is fully charged. A next step in the improvement of HMGS model presented here is thus to include economic gains from injecting the surplus of renewable energy into the public grid. Optimized system results for PV, Wind, Public Grid and Surplus of the generation produced/achieved are shown in Fig. 8.

Both the PV and Wind graphs in Fig. 8(a,b) present the hourly and weekly average generation (black line). PV reaches a maximum generation rate of 140 kW in summer. On the contrary, wind power reaches a maximum output of 240 kW in autumn and winter. The dispersion of wind generation is greater due to the currents of air that occurred during the year in the studied region.

Electricity from the public grid is only used in the HMGS model when demand cannot be covered by renewable sources and BESS, as depicted in Fig. 8(c) (floating average between 20 to 60 kW). The weekly average surplus from renewables with and without BESS is also depicted in Fig. 8(d). The BESS helped reduce the yearly surplus in the HMGS by (36%) from 217 MWh/a to 139 MWh/a.

A sensitivity analysis regarding efficiency and BESS cell cost was carried out to better understand the impact of these characteristics on the HMGS (Fig. 9). It can be clearly seen that both factors have a high impact on HMGS cost. This comes especially true for high BESS costs in combination with low efficiency grades. This underpins the relevance of choosing a suitable BESS for HMGS operation.

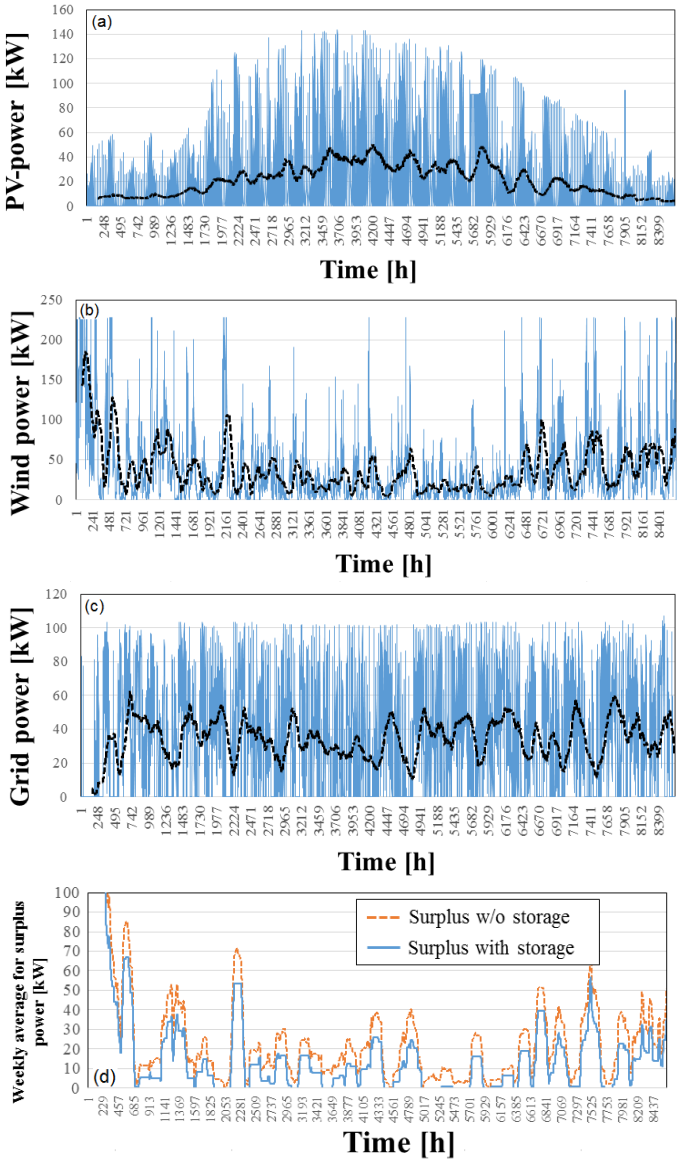

Fig. 8. Electricity generated per hour(h)/year in which source of HMGS model with optimization realized by C-DEEPSO algorithm.

B. BESS evaluation with AHP+TOPSIS

C-DEEPSO algorithm was run 30 times using the initialization parameters presented by Section VI-A in order to optimize the HMGS with different batteries, as described in Section II. Table VI shows the calculated mean values and their standard deviations for RS_{factor} and COE for each tested BESS. LOLP remained very low for all BESS technologies as depicted by Table VI.

The results of the optimization process were used as an input for MCDA. The inquiry for MCDA was carried out in an exploratory way for the three criteria of minimum LOLP and COE, as well as a high RS_{factor}. An AHP Excel-VBA file with an automated GCI based consistency check was distributed among 5 HMGS experts. The expert group

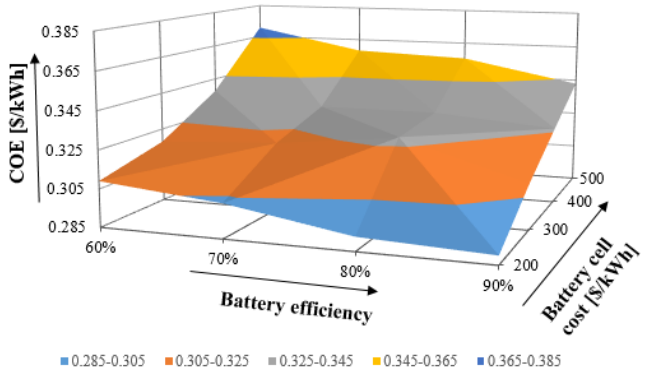

Fig. 9. Operation of a BESS characterizing the load and the discharge of electrical energy in the period of one year.

TABLE VI
OPTIMIZATION RESULTS FOR EACH BESS

	COE ($/kWh)	LOLP (%)	RS_{factor} (%)
VRLA	(0.3139, 0.0029)	(0.0247, 0.0007)	(0.6297, 0.0081)
LFP	(0.3070, 0.0027)	(0.0255, 0.0014)	(0.6343, 0.0130)
NCA	(0.3139, 0.0031)	(0.0247, 0.0013)	(0.6332, 0.0147)
NaNiCl	(0.3066, 0.0014)	(0.0256, 0.0009)	(0.6321, 0.0108)
NaS	(0.3125, 0.0018)	(0.0253, 0.0007)	(0.6318, 0.0129)

consisted of 3 academics from 2 German research centers and 2 experts from a utility and energy consulting company. The participants were supported through the AHP process by explaining the meaning of the criteria and the HMGS model itself. Preferences regarding COE, LOLP and RS_{factor} of the experts are given in Fig. 10.

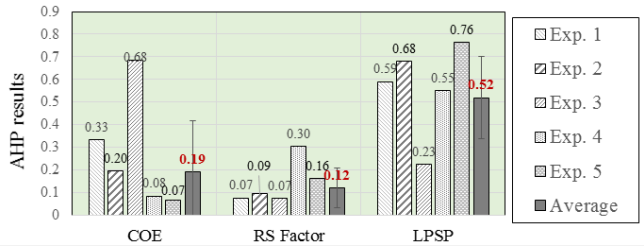

Fig. 10. Obtained single and average weights from HMGS experts.

It can be seen that a low LOLP is considered as the most important factor for HMGS operation by the entire group, followed by a low COE. A high RS_{factor} was weighted the lowest in average. However, priorities are diverse leading to a rather dispersed group decision which has to be considered on the analysis of AHP-results. Experts struggled to attribute weights to LOLP as they thought it would be highly dependent on the type of end-users (e.g. a household is less sensitive to shortage in supply than a small retail business). There is thus some room for refinement for future modeling in HMGS with different kinds of loads (e.g. inclusion of a production line).

Nevertheless, the priorities showed that a low LOLP plays a superior role for most experts in relation to COE and RS-Factor. One exception is expert no. 3 which has a strong preference regarding low COE. AHP results were finally used as input to TOPSIS, in combination with C-DEEPSO results for the three optimization goals to provide a ranking of BESS regarding HMGS requirements for decision support. The score and ranking of batteries for all expert weights and their average are given in Fig. 11.

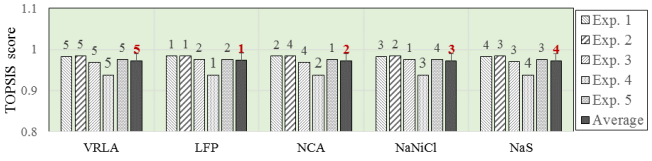

Fig. 11. TOPSIS results based on C-DEEPSO and AHP results.

It can be seen that LFP was ranked first using average weights. This can be explained by the low cost and favorable technical properties of this BESS type. NCA, also a Lithium based BESS type, was in average the second best option. NaNiCl and NaS were ranked on the third and fourth place whereas VRLA was ranked last. The ranking for single experts indicated very different results. This observation is especially true for expert no. 3, who indirectly favored NaNiCl batteries which in average were ranked third. Finally, note that VRLA batteries, which had low cost on the first glimpse, were ranked last in every case due to low cycle life, leading to high cost per conducted cycle and comparably low efficiency rates.

VII. CONCLUSION

In this paper, very different BESS (Lithium Iron Phosphate - LFP, Lithium Nickel Cobalt Aluminum Oxide - NCA, lead acid, Sodium Sulfur - NaS and Sodium Nickel Chloride batteries - NaNiCl) were analyzed regarding their suitability for HMGS operation. A HMGS-optimization model was used to minimize overall system cost, electrical losses, and to increase the maximum use of local available renewable sources (wind and solar power) by simultaneously reducing electricity consumption from the public grid. An algorithm called C-DEEPSO was tested to carry out the electrical dispatch and to provide an optimum allocation of generation capacities. The results showed that the applied evolutionary method provided satisfactory control to electric dispatch and design of the microgrid system. After this, further experiments were conducted to test each BESS regarding its impact on the three different HMGS optimization goals.

The results for the three optimization goals were used as inputs to a multi-criteria decision analysis process to provide a ranking of the most suitable HMGS storage alternative. The Analytic Hierarchy Process was used to gather the preferences of five experts from the area. Aggregation of inputs was carried out with the Technique for Order Preference by Similarity to Ideal Solution (TOSPSIS). Results indicated that LFP and NCA provided the most benefits, followed by NaNiCl. NaS and VRLA did not seem to be recommendable for the HMGS case analyzed. In addition, this analysis revealed that the group decision is dispersed, indicating that more participants and discussions are required for further research. Finally, it is worth mentioning that the size of BESS and the marketing of excess energy have not been included as goals in the optimization model. Note that these goals can be easily included into the model by representative weights for the respective objective functions, which would allow to choose the adequate size for the BESS based on the results of AHP.

ACKNOWLEDGMENT

The authors would like to thank CEFET-MG, INESC TEC, UNL, KIT and ITAS for the infrastructure used by this project and to thank also CAPES, CNPq, FAPEMIG and FAPERJ for the financial support. This work is financed by the BE MUNDUS project and the Helmholtz-Project Energy System 2050.

REFERENCES

[1] AGUARON, J., AND MORENO-JIMENEZ, J. M. The geometric consistency index: Approximated thresholds. *Eur. J. Oper. Res., vol. 147, pp. 137-145, May* (2003).

[2] BARELLI, L., BIDINI, G., AND BONUCCI, F. A microgrid operation analysis for cost-effective battery energy storage and RES plants integration. *Energy, vol. 113, pp. 831-844* (2016).

[3] BAUMANN, M., PETERS, J., WEIL, M., AND GRUNWALD, A. CO2 footprint and life cycle costs of electrochemical energy storage for stationary grid applications. *Energy Technology, no. Submitted* (2016).

[4] BAUMANN, M., PETERS, J., WEIL, M., MARCELINO, C., ALMEIDA, P., AND WANNER, E. Environmental impacts of different battery technologies in renewable hybrid micro-grids. In *accepted: IEEE International Conference on Innovative Smart Grid Technologies, Torino, Italy* (2017).

[5] BORHANAZAD, H., MEKHILEF, S., GANAPATHY, V., MODIRI-DELSHAD, M., AND MIRTAHERI, A. Optimization of micro-grid system using MOPSO. *Renewable energy, Vol. 71, pp. 295-306* (2014).

[6] CARVALHO, L., LOUREIRO, F., SUMALI, J., KEKO, H., MARCELINO, C., WANNER, E., AND MIRANDA, V. Statistical Tuning of DEEPSO Soft Constraints in the Security Constrained Optimal Power Flow Problem. In *Proc: in 18th International Conference on Intelligent System Application to Power Systems (ISAP), pp. 1-8* (2015).

[7] CHEN, H., CONG, T. N., YANG, W., TAN, C., LI, Y., AND DING, Y. Progress in electrical energy storage system: A critical review. *Prog. Nat. Sci., vol.19,pp. 291-312* (2009).

[8] COELLO, C., LAMONT, G., DAVID, A., AND VELDHUIZEN, V. *Evolutionary Algorithms for Solving Multi-Objective problems*. 2th Edition, 2007.

[9] CRAWFORD, G. The geometric mean procedure for estimating the scale of a judgement matrix. *Math. Model., vol. 9, no. 3–5, pp. 327-334* (1987).

[10] DWD. Deutscher Wetterdienst: Wetter und Klima aus einer Hand. Tech. rep., Deutscher Wetterdienst: Wetter und Klima aus einer Hand, Available: http://www.dwd.de/DE/leistungen/windkarten/windkarten.html. [Accessed: 01-Feb-2018]., 2018.

[11] EHRGOTT, M. A discussion of scalarization technics for multiple objective interger programming. *Annals of Operations Research, vol. 147, pp: 343-460* (2006).

[12] EICHFELDER, G. *Adaptative Scalarization Methods in a Multiobjective Optimization*. 1th edition, 2008.

[13] FARHANGI, H. The path of the smart grid. *IEEE Power Energy Mag., vol. 8, no. 1, pp. 1828* (2010).

[14] GAMPE, D. Kleinwindkraftanlagen Hintergrundinformationen und Handlungsempfehlungen für die Landwirtschaft. *Centrales Agrar, Straubing* (2013).

[15] GARCIA-CASCALESA-CASCALES, M. S., AND LAMATA, M. T. On rank reversal and TOPSIS method. *Math. Comput. Model., vol. 56, no. 5-6, pp. 123-132, Sep* (2012).

[16] GOODWIN, P. *Decision analysis for management judgment*. 3rd ed. Hoboken, 2004.

[17] GUITOUNI, A., AND MARTEL, J.-M. Tentative guidelines to help choosing an appropriate MCDA method. *Eur. J. Oper. Res., vol. 109, no. 2, pp. 501-521* (1998).

[18] HWANG, C.-L., AND YOON, K. Multiple attribute decision making: methods and applications; a state-of-the-art-survey. *Berlin: Springer, 1981* (1981).

[19] J., O. Multikriterielle Bewertung von Technologien zur Bereitstellung von Strom und Wärme. *Universitat Gottingen, Gottingen* (2010).

[20] KAABECHE, A., BELHAMEL, M., AND IBITIOUEN, R. Techno-economic valuation and optimization of integrated photovoltaic/Wind energy conversion system. *Solar Energy, 85(10):2407-2420* (2011).

[21] KAVIANI, A., RIAHY, G., AND KOUHSARI, S. Optimal design of a reliable hydrogen-based stan-alone wind/PV generating system, considering component outages. *Renewable Energy, Vol. 34, pp. 2380-2390* (2009).

[22] KAZMI, S. A., HASAN, S. F., AND SHIN, D.-R. Multi Criteria Decision Analysis for Optimum DG Placement in Smart Grids. *Proc.in: IEEE ISGT, pp:1-5* (2015).

[23] KEMPTIN, W., AND TOMIC, J. Vehicle-to-grid power fundamentals: calculating capacity and net revenue. *Journal of power Sources, v. 144, pp: 268-279* (2005).

[24] LEVRON, Y., GUERRERO, J. M., AND BECK, Y. Optimal Power Flow in Microgrids With Energy Storage. *IEEE Trans. Power Syst., vol. 28, no. 3, pp. 3226-3234, Aug* (2013).

[25] MAJUMDER, M. Multi Criteria Decision Making. *Impact of Urbanization on Water Shortage in Face of Climatic Aberrations, Singapore: Springer Singapore, pp. 35-47* (2015).

[26] MARCELINO, C., BAUMANN, M., WEIL, M., CARVALHO, L., WANNER, E., ALMEIDA, P., AND MIRANDA, V. Solving security constrained optimal power flow problems: a hybrid evolutionary approach. *Applied Intelligence, pp.: 1-19* (2018).

[27] MIETTINEN, K., AND MAKELA, M. On scalarizing functions in a multiobjective optimization. *OR Spectrum, v. 24, pp: 193-213* (2002).

[28] MIRANDA, V., KEKO, H., AND DUQUE, A. Stochastic star communication topology in evolutionary particle swarms (epso). *International Journal of Computational Intelligence Research. ISSN 0973-1873 Vol.4, No.2, pp.105-116* (2008).

[29] MOGHADDAM, A., SEIFI, A., NIKNAM, T., AND PAHLAVANI, M. Multi-objective operation management of a renewable MG (micro-grid) with back-up micro-turbine/fuel cell/battery hybrid power source. *Energy, Elsevier, vol 36, pp: 6490-6507* (2011).

[30] MOHAMMADI, M., HOSSEINIAN, S., AND GHAREHPETIAN, G. Optimization of hybrid solar energy sources/wind turbine systems integrated to utility grids as microgrid (MG) under pool/bilateral/hybrid market using PSO. *Solar Energy, pp: 112-125* (2012).

[31] PEREIRA, V., SOUZA, P., CORTEZ, P., RIO, M., AND

ROCHA, M. Comparasion of Single and Multi-objective Evolutionary Algorithm for Robust Link-State Routig. *Lecture Notes on Computer Science, Part II, vol 9019, pp: 573-587* (2015).

[32] PERERA, N., AND SUTRISNA, M. The Use of Analytic Hierarchy Process (AHP) in the Analysis of Delay Claims in Construction Projects in the UAE. *Built Hum. Environ. Rev., vol. Volume 3, no. Special Issue 1, pp. 29-48* (2010).

[33] SAATY, R. W. The analytic hierarchy process-what it is and how it is used. *Math. Model., vol. 9, no. 3–5, pp. 161-176* (1987).

[34] SAATY, T. L. The analytic hierarchy process: planning, priority setting, resource allocation. *PA: RWS Publications* (1990).

[35] SODA. Time Series of Solar Radiation Data - for Free, 2016. Tech. rep., Available: http://www.soda-is.com/eng/index.html.[Accessed: 08-May-2016]., 2016.

[36] STENZEL, P., BAUMANN, M., AND FLEER, J. Database development and evaluation for techno-economic assessments of electrochemical energy storage systems. *Proc. in: ENERGYCON, pp.: 1334-1342* (2014).

[37] STORN, R., AND PRICE, K. Differential Evolution: a simple and efficient adaptative scheme for global optimization over continuous spaces. *Techinical report TR-95-012, ICSI, Berkley* (1995).

[38] SULLIVAN, J., AND GAINES, L. A Review of Battery Life Cycle Analysis: State of Knowledge and Critical Needs. *Argonne National laboratory, Oak Ridge* (2010).

[39] VASILJEVSKA, J., LOPES, J., AND MATOS, M. Evaluating the impacts of the multi-microgrid concept using multicriteria decision aid. *Electric Power System Research, pp: 44-51* (2012).

[40] WANG, Y.-M., AND LUO, Y. On rank reversal in decision analysis. *Math. Comput. Model., vol. 49, no. 5–6, pp. 1221-1229, Mar.* (2009).

[41] WIMMLER, C., HEJAZI, G., FERNANDES, E., MOREIRA, C., AND CONNORS, S. Multi-Criteria Decision Support Methods for Renewable Energy Systems on Islands. *J. Clean Energy Technol., vol. 3, pp. 185-195* (2015).

[42] ZAIDAN, A., ZAIDAN, B. B., AL-HAIQI, A., KIAH, M. L. M., HUSSAIN, M., AND ABDULNABI, M. Evaluation and selection of open-source EMR software packages based on integrated AHP and TOPSIS. *J. Biomed. Inform., vol. 53, pp. 390-404, Feb.* (2015).